Eksakta : Berkala Ilmiah Bidang MIPA
VOLUME 27 NO 05 2026, pp 871-883
ISSN : Print 1411-3724 — Online 2549-7464
DOI : https://doi.org/10.24036/eksakta/vol27-iss05/741

Eksakta
Berkala Ilmiah Bidang MIPA
http://www.eksakta.ppj.unp.ac.id/index.php/eksakta

Article

Multidimensional Drought Intensification in Banjar Regency: A Combined Drought Index and Spatial Regression Assessment

Henyningtyas Suhel[1*], Arif Eko Wibawanto[1]

[1]Bachelor of Applied Geomatics and Survey Engineering Technology Study Program, Department of Civil Engineering and Earth Sciences, Politeknik Negeri Banjarmasin, Banjarmasin, Indonesia

Article Info

Article history :
Received August 08, 2026
Revised September 30, 2026
Accepted October 07, 2026
Published October 30, 2026

Keywords :
Drought monitoring,
composite index,
spatial regression,
google earth engine,
South Kalimantan

Abstract. Drought in humid tropical landscapes emerges from interacting rainfall, soil moisture, vegetation, surface-water, and thermal stress. This study assessed dry-season drought in Banjar Regency, South Kalimantan, for 2015 and 2025 and examined a 2025–2031 sensitivity scenario based on an assumed 1.5% decline in soil moisture, 3.0% increase in land surface temperature, and unchanged NDVI. A Combined Drought Index (CDI) integrated CHIRPS rainfall, GLDAS soil moisture, Landsat NDVI, MNDWI, and land surface temperature using Analytical Hierarchy Process weights. The CDI range shifted from 0.356–0.761 in 2015 to 0.601–0.853 in 2025, with persistent high-stress conditions in western lowlands and broader moderate stress across the central corridor. OLS residuals showed strong spatial autocorrelation, while GWR increased R^2 to 0.982 and 0.988 and reduced AICc, indicating spatially varying component-index relationships. The sensitivity scenario suggests increasing vulnerability where thermal stress rises and soil moisture declines. Management should therefore prioritize wetland retention and soil-water conservation in the western districts, irrigation and surface-water management in the central corridor, drought-sensitive agricultural planning in the north, and forest-catchment protection in the eastern districts.

This is an open acces article under the CC-BY license.

This is an open access article distributed under the Creative Commons 4.0 Attribution License, which permits unrestricted use, distribution, and reproduction in any medium, provided the original work is properly cited. ©2026 by author.

Corresponding Author :
Henyningtyas Suhel
Bachelor of Applied Geomatics and Survey Engineering Technology Study Program, Department of Civil Engineering and Earth Sciences, Politeknik Negeri Banjarmasin, Banjarmasin, Indonesia
Email : heny.ningtyas@poliban.ac.id

1. Introduction

Drought is not simply a shortage of rain. It is a cascading disturbance that connects atmospheric deficits with soil-water depletion, vegetation stress, thermal anomalies, reduced surface-water availability, and eventually social and economic disruption. Recent research therefore treats drought as a multidimensional risk whose severity depends on interacting biophysical pressures and the ability of landscapes and communities to absorb water stress [1-4]. This perspective is especially important in humid tropical regions, where the expectation of abundant rainfall can obscure seasonal and locally intensified drought until ecological and livelihood impacts are already emerging.

Banjar Regency in South Kalimantan presents a demanding setting for drought assessment. Its landscape transitions from western lowlands, tidal and inland wetlands, agricultural areas, and peat-influenced terrain toward the forested hills of the Meratus system in the east. Local evidence confirms the importance of peatland and seasonal water availability in the western part of the regency. A study in Gambut District documented shallow peatland conditions and examined daily groundwater-table elevation during the June–August 2022 dry-season period, demonstrating the hydrological sensitivity of this landscape [5]. Historical drought and fire evidence also indicates that Gambut District experienced severe peatland drought conditions and substantial fire activity in 2014, 2015, and 2019, with 357 hotspots recorded in 2015 and 233 in 2019 [6].

In addition, official regional planning data report 720.11 ha of forest and land fires across several Banjar districts in 2018, including Gambut, Sungai Tabuk, Martapura Barat, and Karang Intan. These observations support the characterization of the western lowlands as environmentally sensitive wetland and peat-influenced landscapes. Land-use change in Banjar Regency and neighboring Banjarbaru has also been linked to agricultural and plantation expansion, indicating that local hydrologic behavior increasingly reflects interactions between climate variability and human modification of the landscape [7]. In such settings, drought risk cannot be inferred from precipitation alone. Rainfall deficits may be amplified by low soil moisture, exposed or built surfaces, weakened wetland storage, and elevated land surface temperature, whereas forested or water-retentive landscapes may buffer part of the stress.

Remote sensing provides a practical way to observe these interactions over large and heterogeneous areas. Recent composite approaches combine precipitation, vegetation, thermal, and soil-moisture information because individual indicators respond to different stages of drought and may produce misleading signals when used alone [8-13]. For example, low vegetation greenness can reflect harvest or land-cover change rather than drought, while high surface temperature may be associated with built-up land as well as moisture stress. Google Earth Engine further supports operational drought assessment by allowing multisensor and multitemporal datasets to be processed efficiently at regional scales [14-15].

A second challenge is spatial non-stationarity. The same change in soil moisture, rainfall, or temperature may not have an identical association with drought conditions in wetlands, peri-urban zones, irrigated agricultural corridors, and forested uplands. Recent drought studies have therefore used geographically weighted approaches to reveal local relationships that are hidden by global regression [16-18]. Related work on soil-moisture downscaling also shows that vegetation and thermal controls can operate at different spatial scales [19-21]. These findings argue against relying on a single regional coefficient when the management problem itself is spatially differentiated.

This study integrates five biophysical dimensions into a Combined Drought Index (CDI) for Banjar Regency, compares peak dry-season conditions in 2015 and 2025, diagnoses spatial dependence in a global regression, and applies Geographically Weighted Regression (GWR) to describe local attribution patterns. A scenario-based sensitivity analysis is then used to explore how higher land surface temperature and lower soil moisture could redistribute vulnerability through 2031. The study is intentionally interpretive rather than causal. Because the CDI is mathematically

constructed from the same environmental components later entered into the regression, GWR is used to reveal where component-index relationships vary spatially, not to claim independent prediction or causal effects. This distinction is necessary when interpreting the spatial regression results. Furthermore, the comparison between 2015 and 2025 represents two selected dry-season states under different climatic and environmental conditions rather than a continuous temporal series. Therefore, the observed difference in CDI values should not be interpreted as evidence of a linear decade-long drought intensification or as a direct measure of climate-change effects.

2. Method

This study integrates five biophysical dimensions into a Combined Drought Index (CDI) for Banjar Regency, compares selected peak dry-season conditions in 2015 and 2025 under different large-scale climate backgrounds, diagnoses spatial dependence in a global regression, and applies Geographically Weighted Regression (GWR) to describe local attribution patterns. A scenario-based sensitivity analysis is then used to explore how higher land surface temperature and lower soil moisture could redistribute vulnerability through 2031. The comparison is intended to identify spatial differences between two selected dry-season states rather than infer a linear temporal trend in drought or climate change.

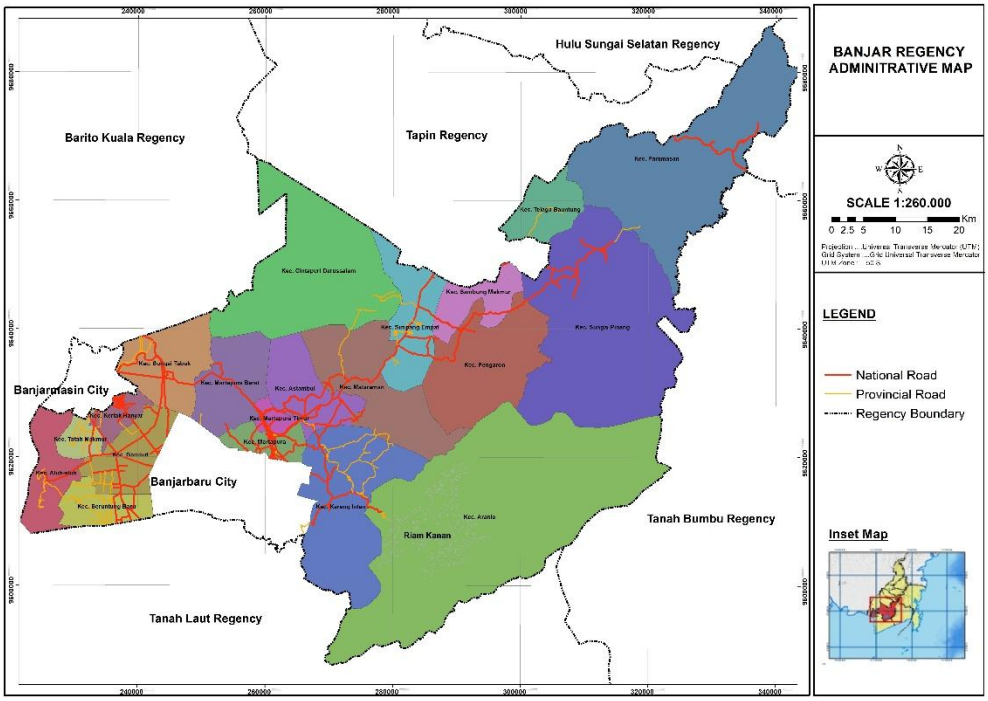


Figure 1. Administrative context and study area of Banjar Regency, South Kalimantan, Indonesia

All raster data were acquired and processed in Google Earth Engine. Monthly rainfall was obtained from CHIRPS at 0.05 degree resolution. Surface soil moisture was obtained from the GLDAS Noah land-surface model at 0.25 degree resolution for the 0–10 cm layer. NDVI and MNDWI were derived from Landsat 8 OLI surface reflectance for 2015 and Landsat 9 OLI-2 surface reflectance for 2025 after QA_PIXEL cloud masking. Land surface temperature was derived from Landsat thermal observations within the GEE workflow using the [INSERT ACTUAL LST ALGORITHM] algorithm. The LST retrieval followed the formulation described by [INSERT LST REFERENCE], with the resulting temperature values converted to degrees Celsius before spatial

aggregation. The use of multisource information is consistent with recent evidence that integrated drought indicators are generally more robust than single-variable measures because precipitation, soil moisture, vegetation, and temperature capture different parts of drought propagation [22-26].

Table 1. Environmental inputs used to construct the Combined Drought Index.

Variable	Source and Nominal Resolution	Role in CDI	Reported Drought Relation
Rainfall	CHIRPS monthly, 0.05 degree	Meteorological water supply	Lower values indicate greater stress
Soil moisture	GLDAS Noah 0-10 cm, 0.25 degree	Near-surface water availability	Lower values indicate greater stress
NDVI	Landsat 8/9 surface reflectance, 30 m	Vegetation condition	Lower values indicate greater stress
MNDWI	Landsat 8/9 surface reflectance, 30 m	Surface-water and wetness signal	Lower values indicate greater stress
LST	Landsat 8/9 thermal data, 30 m	Thermal stress	Higher values indicate greater stress

Because the input datasets had different spatial resolutions, a common spatial framework was required before constructing the CDI. The Landsat-derived NDVI, MNDWI, and LST layers had a nominal resolution of 30 m, whereas CHIRPS rainfall and GLDAS soil moisture had substantially coarser spatial resolutions. The input layers were therefore harmonized to the 1 km × 1 km analysis grid using [INSERT ACTUAL RESAMPLING METHOD] before the CDI calculation. The 1 km grid was used as the common spatial support for all variables, while the original nominal resolutions of the source datasets were retained for data acquisition and preprocessing. In particular, the 1 km grid should be interpreted as an analysis grid rather than as a downscaled representation of the native 0.25° GLDAS observations.

Table 2. AHP weights used in the Combined Drought Index.

Component	Weight	Interpretive Role
Rainfall	0.35	Primary atmospheric water input
Soil moisture	0.25	Direct soil-water stress proxy
LST	0.18	Thermal stress and evaporative demand proxy
NDVI	0.12	Vegetation response
MNDWI	0.10	Surface-water and wetness response

CDI and the five environmental inputs were summarized to a 1 km by 1 km fishnet grid covering the regency. Because the input datasets had different spatial resolutions, all environmental layers were harmonized to a common 1 km × 1 km analysis grid before CDI construction. The Landsat-derived variables had a nominal spatial resolution of 30 m, whereas CHIRPS rainfall and GLDAS soil moisture were available at substantially coarser resolutions. The layers were resampled to the 1 km analysis grid using the bilinear method prior to grid-level aggregation. The 1 km grid represents the common spatial support for analysis rather than a downscaled representation of the native GLDAS

observations. A global Ordinary Least Squares (OLS) model was first estimated with CDI as the dependent variable and the five component variables as predictors. Global Moran's I was calculated on OLS residuals to test whether unexplained values remained spatially clustered. The Studentized Breusch-Pagan test was used to diagnose heteroscedasticity.

These tests address different assumptions: Moran's I indicates spatial dependence in the residual pattern, whereas Breusch-Pagan indicates nonconstant residual variance and is not, by itself, a test of spatial non-stationarity. GWR was then fitted to allow coefficients to vary by geographic location, following the logic of spatially varying relationships [16]. Model comparisons used R^2, adjusted R^2, and corrected Akaike Information Criterion (AICc). Because CDI is a weighted composite of the same environmental components, the regressions are treated as a spatial attribution and reconstruction exercise rather than independent predictive validation.

A 2025–2031 sensitivity scenario was implemented in Python using controlled perturbations of the environmental components, assuming no change in NDVI, a 1.5% decline in soil moisture, and a 3.0% increase in LST. These values were specified as bounded perturbations for an empirical stress test rather than as projections derived from a climate model or climate-change scenario. The purpose of the scenario was to examine the spatial sensitivity of CDI to changes in two key drought-stress components, namely soil moisture and land surface temperature. Accordingly, the resulting map does not represent a probabilistic prediction of actual drought conditions in 2031, but rather a conditional assessment of how drought vulnerability could change if the specified perturbations occurred. Recent spatially adaptive drought projections demonstrate the value of local modeling while also highlighting the importance of multiple climate scenarios and uncertainty ranges for future projections [27].

3. Results and Discussion

The CDI mapped a marked shift in the drought baseline between the two observation years. In 2015, CDI values ranged from 0.356 to 0.761. High reported drought values were concentrated in the western and northwestern lowlands, including Cintapuri Darussalam, Sungai Tabuk, Kertak Hanyar, Gambut, Tatah Makmur, Aluh-Aluh, Beruntung Baru, and Martapura Barat. The central and eastern portions of the regency, including much of Aranio and Paramasan, remained comparatively less stressed. This spatial contrast is consistent with multidimensional drought monitoring, in which rainfall deficits become more consequential where low soil moisture, surface-water loss, and high thermal load reinforce one another [8], [10-11].

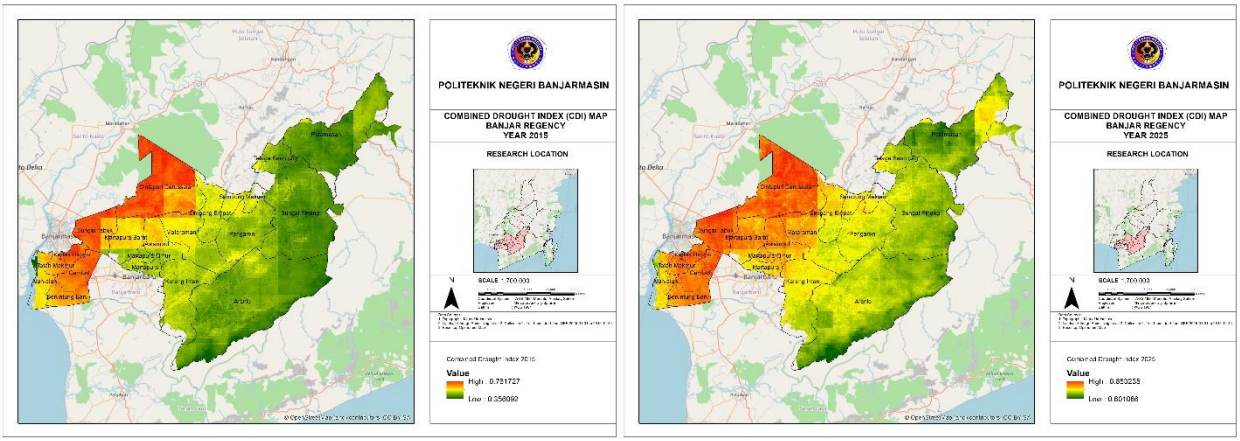


Figure 2. Combined Drought Index for the August to October observation windows in (a) 2015 and (b) 2025.

By 2025, the reported CDI range shifted upward to 0.601-0.853. The increase in the minimum value is more informative than the change in the maximum alone because it suggests that areas previously classified as comparatively wet moved toward moderate stress. Western lowland districts remained the most consistently exposed, while moderate conditions expanded through the central corridor, including Simpang Empat, Mataraman, Astambul, Martapura, Martapura Timur, and parts of Karang Intan. Eastern districts such as Aranio, Sungai Pinang, Telaga Bauntung, and Paramasan still showed the lowest CDI values in the regency, although their relative buffer weakened compared with 2015.

This pattern should not be interpreted as proof of a monotonic ten-year climatic trend because the design compares only two selected seasonal snapshots. It does, however, identify a spatial redistribution that is operationally meaningful. The western zone combines low elevation, wetland and agricultural land uses, peri-urban expansion, and surfaces that can experience strong thermal loading. The eastern landscape contains more forest and topographic water-storage functions. Land-use change research in Banjar Regency adds an important human dimension because changes in agricultural and plantation land use can alter runoff, infiltration, vegetation cover, and landscape water retention, shaping how the same climatic signal is experienced locally [7]. In practical terms, the CDI map is not only a climate map. It also reflects the surfaces that communities farm, drain, build on, and depend on.

An important limitation of the present analysis is the absence of direct external validation of the Combined Drought Index (CDI) against independent field-based or impact observations. The OLS and GWR analyses presented in this study should not be considered external validation because the dependent variable, CDI, is mathematically constructed from the same environmental components subsequently used as explanatory variables. Consequently, the high explanatory performance of GWR reflects the spatial reconstruction of the composite index rather than an independent test of its predictive validity.

Nevertheless, the spatial patterns identified by the CDI are broadly consistent with independent evidence of environmental sensitivity in Banjar Regency. Previous observations have documented forest and land fires in several western and central districts, including Gambut, Sungai Tabuk, Martapura Barat, and Karang Intan. These areas overlap with portions of the western lowland zone that exhibit relatively high CDI values in the present study. Such correspondence provides contextual support for the interpretation that the western lowlands represent environmentally sensitive areas, although it cannot be interpreted as a statistical validation of the CDI.

The CDI results should therefore be interpreted primarily as a spatial screening and attribution framework. The upward shift in the CDI range from 0.356–0.761 in 2015 to 0.601–0.853 in 2025 indicates differences between the two selected dry-season states, while the persistence of high-stress areas in the western lowlands and the expansion of moderate stress toward the central corridor identify locations that warrant closer monitoring. However, without an independent dataset, the magnitude and classification performance of CDI cannot be quantitatively evaluated.

Future validation should compare CDI with independent observations, such as BMKG station-based rainfall and derived SPI/SPEI, documented drought or forest-fire events from local disaster-management agencies, agricultural production losses, or other field observations. Such comparisons would allow the direction, strength, and statistical significance of the CDI–impact relationship to be evaluated independently and would provide a stronger basis for assessing the operational reliability of the index. Recent composite-index studies similarly emphasize validation against independent drought indices, crop outcomes, or field observations [9], [13], [18], [23].

The global OLS residuals were strongly spatially structured. Moran's I was 0.6681 in 2015 and 0.8231 in 2025, with $p < 2.2 \times 10^{-16}$ in both years. The increase of approximately 0.155 indicates stronger positive residual clustering in 2025. The Moran scatterplots were dominated by High-High

and Low-Low configurations, showing that neighboring grid cells tended to share similar residual behavior rather than fluctuate randomly. This pattern violates the spatial-independence expectation of a purely global model and supports a local modeling framework.

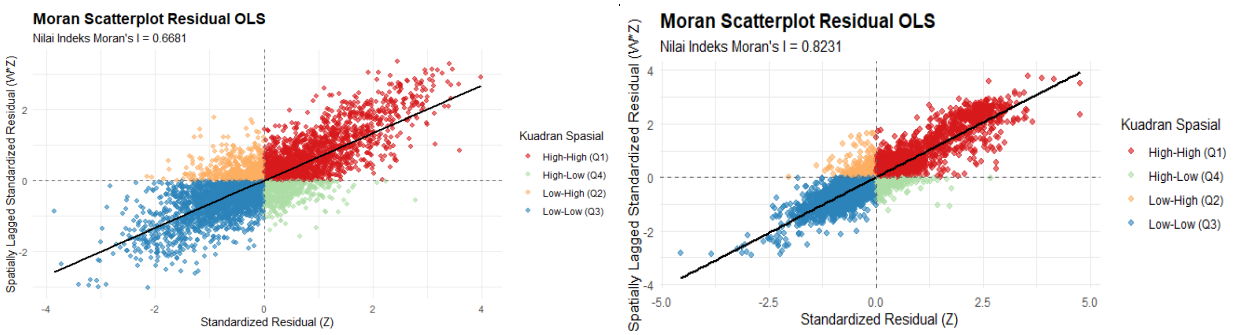


Figure 3. Moran scatterplots of OLS residuals for (a) 2015 and (b) 2025, showing strong positive spatial autocorrelation.

The Studentized Breusch-Pagan test also rejected homoscedasticity for both periods, with statistics of 653.81 in 2015 and 188.89 in 2025 ($df = 5$, $p < 0.001$). The larger 2015 statistic suggests stronger nonconstant variance in that cross-section, but it should not be labeled direct evidence of spatial non-stationarity. Taken together, residual spatial autocorrelation, heteroscedasticity, and visible geographic contrasts justify examining location-dependent coefficients. This interpretation is consistent with recent drought modeling in which geographically weighted approaches captured local relationships that were suppressed in global formulations [16-17].

GWR produced a much stronger in-sample fit than OLS in both years. R^2 increased from 0.9260 to 0.9816 in 2015 and from 0.8620 to 0.9875 in 2025. Adjusted R^2 showed the same pattern, while AICc decreased sharply. The spatial distribution of local R^2 was also informative. In 2015, the highest local fit was concentrated mainly in western and central zones. By 2025, high local R^2 values were more widespread, including parts of the north and east. This indicates that a local coefficient structure reconstructed the CDI surface more consistently across the regency than a single global equation.

Table 3. Comparison of global OLS and local GWR model performance.

Metric	OLS 2015	GWR 2015	OLS 2025	GWR 2025
R^2	0.9260	0.9816	0.8620	0.9875
Adjusted R^2	0.9260	0.9782	0.8620	0.9854
AICc	-24,240.00	-29,380.51	-26,310.00	-36,598.05

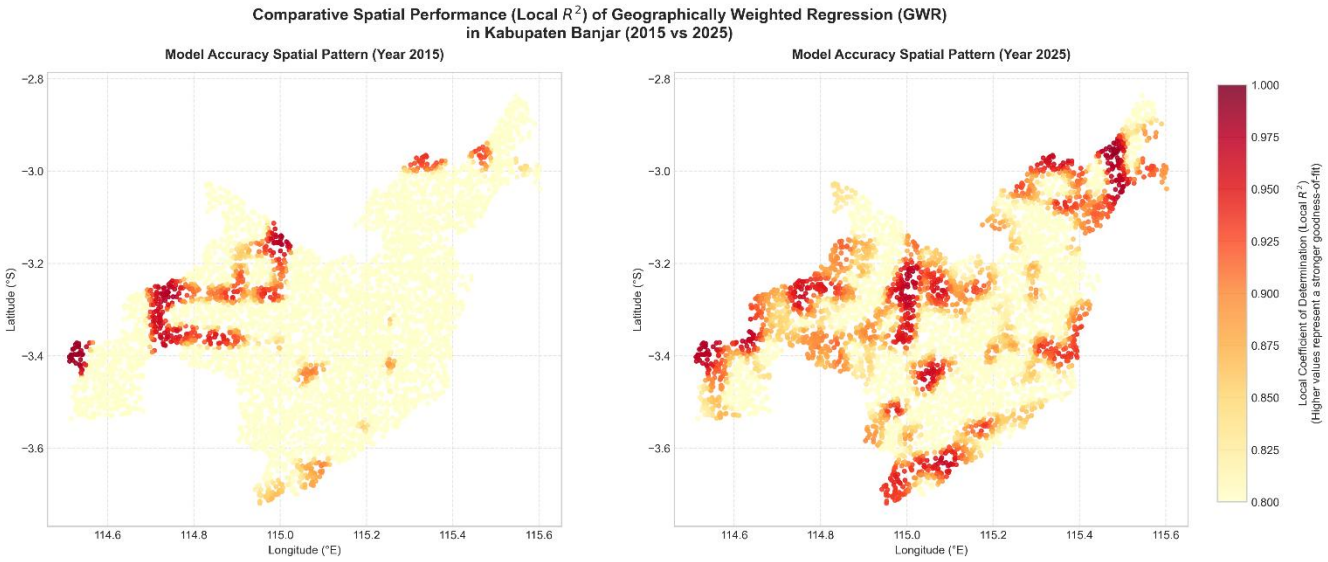


Figure 4. Spatial distribution of local GWR R² in 2015 and 2025. Higher values indicate stronger local reconstruction of the CDI surface.

The numerical improvement is substantial, but a critical caveat is essential. The dependent variable, CDI, is itself a weighted combination of rainfall, soil moisture, LST, NDVI, and MNDWI. Regressing CDI on those same components therefore creates structural circularity. High R² values are partly expected because the predictors mathematically constitute the outcome. The GWR analysis remains useful for identifying where component-index relationships differ after spatial weighting, scaling, and local covariance are considered, but it cannot serve as independent validation of drought severity. More defensible validation would compare CDI against variables not used to construct it, such as station-based SPEI or SPI, groundwater levels, streamflow, crop-yield anomalies, burned area, field soil moisture, or documented drought impacts. Recent integrated-index studies increasingly use external benchmarks for this purpose [8], [11], [28-29].

The local coefficient maps indicate that modeled contributions were not spatially uniform. The western lowlands were characterized by strong thermal and soil-moisture signals, the central corridor by rainfall and surface-wetness signals, the north by vegetation and rainfall, and the east by surface wetness and vegetation. These patterns are more useful as a management typology than as a ranking of universal causal drivers. Raw GWR coefficients are scale-dependent, so a coefficient for soil moisture cannot be compared directly with a coefficient for LST unless predictor scales are standardized. The interpretation therefore emphasizes mapped local sensitivity and landscape context rather than absolute coefficient magnitude.

Table 4. Spatial attribution patterns and practical management relevance

Spatial Cluster	Prominent Modeled Signals	Management Relevance
West: Gambut, Kertak Hanyar, Aluh-Aluh, Beruntung Baru, Sungai Tabuk	LST and soil moisture	Protect wetland retention, reduce drainage stress, maintain soil moisture, and limit heat-amplifying land conversion.
Center: Martapura, Martapura Barat/Timur, Astambul, Mataraman, Karang Intan	Rainfall and MNDWI	Coordinate irrigation timing, local retention, canal management, and dry-season water allocation.
North: Simpang Empat, Sambung Makmur, Pengaron	NDVI and rainfall	Use crop calendars, drought-tolerant practices, and vegetation-based early-warning indicators.
East: Aranio, Sungai Pinang, Paramasan	MNDWI and NDVI	Protect forest-water connectivity and preserve catchment storage functions around the Riam Kanan system.

The broader implication is that a regency-wide drought policy based on one trigger would be inefficient. A temperature threshold that is informative in the western peri-urban and wetland zone may be less useful in forested eastern catchments, where canopy condition and surface-water continuity better capture resilience. Conversely, a vegetation-only indicator may miss early soil-water depletion in the west. Multisensor monitoring is valuable precisely because different communities and ecosystems experience drought through different pathways. A human-centered interpretation therefore asks what the spatial statistics mean for people, farms, wetlands, and water systems in each location, rather than treating the regency as a uniform surface.

Under the imposed scenario of unchanged NDVI, a 1.5% decline in soil moisture, and a 3.0% increase in LST, the projected change surface suggests relatively stronger buffering in parts of the west and increasing vulnerability across substantial central and eastern areas. The map indicates that thermal increase and soil-moisture loss can overwhelm the assumed stability of vegetation where water retention is less able to compensate. It also illustrates a counterintuitive point: present-day lower vulnerability does not guarantee future resilience if the variables that currently provide buffering are themselves stressed.

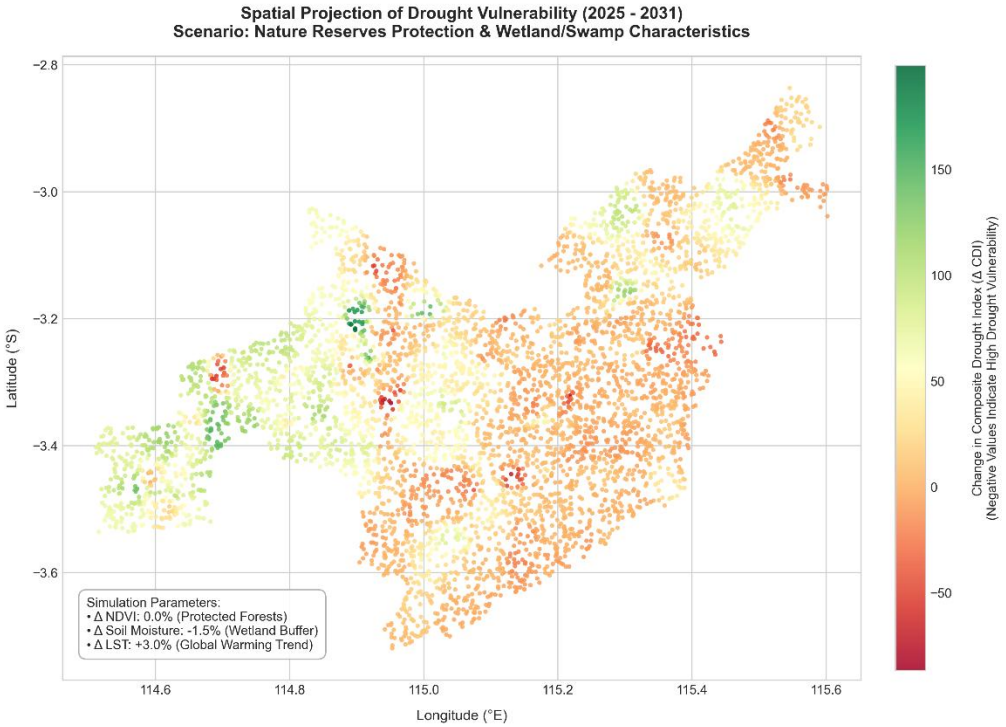


Figure 5. Scenario-based spatial sensitivity of drought vulnerability for 2025-2031 under the imposed changes in soil moisture and land surface temperature.

These results should be used for planning stress tests rather than prediction. The scenario does not incorporate climate-model ensembles, uncertainty ranges, alternative precipitation pathways, groundwater dynamics, evapotranspiration, or future land-use change. Recent spatial drought projection studies show that scenario uncertainty and locally adaptive models can materially change hotspot identification [4], [27], [30]. A stronger future assessment of Banjar Regency should combine the present CDI framework with multiple climate scenarios, longer annual time series, groundwater and evapotranspiration data, and independent impact validation. That extension would turn a useful spatial screening tool into a more defensible decision-support system.

4. Conclusion

The integrated analysis identifies substantial spatial differences in drought stress across Banjar Regency between the selected 2015 and 2025 dry-season observations. The CDI range shifted from 0.356–0.761 in 2015 to 0.601–0.853 in 2025, with persistent high-stress conditions in the western lowlands and broader moderate stress across the central corridor. Rainfall and soil moisture received the largest AHP weights, while the spatial regression results indicate that the relationships between the component variables and CDI vary across the regency. The GWR results provide evidence of spatial non-stationarity but should be interpreted as spatial attribution rather than causal inference or independent validation because CDI was constructed from the same environmental components used in the regression. Similarly, the 2025–2031 analysis represents a conditional sensitivity scenario based on imposed changes in soil moisture and land surface temperature, rather than a deterministic climate projection.

The main practical contribution of the study is a spatial screening framework that can support differentiated drought management, including wetland and soil-water retention in western areas, irrigation and surface-water management in the central corridor, drought-sensitive agricultural planning in the north, and forest-catchment protection in the east. However, the absence of independent field or impact observations limits quantitative assessment of CDI validity. Future research should therefore validate CDI against independent meteorological, hydrological, agricultural, or disaster-impact observations and extend the analysis using longer time series and multiple climate scenarios.

References

[1] Jiao, W., Wang, L., & McCabe, M. F. (2021). Multi-sensor remote sensing for drought characterization: current status, opportunities and a roadmap for the future. *Remote Sensing of Environment*, *256*, 112313.

[2] Rahman, G., Jung, M. K., Kim, T. W., & Kwon, H. H. (2025). Drought impact, vulnerability, risk assessment, management and mitigation under climate change: A comprehensive review. *KSCE Journal of Civil Engineering*, *29*(1), 100120.

[3] Serkendiz, H., Tatli, H., Özcan, H., Cetin, M., & Sungur, A. (2023). Multidimensional assessment of agricultural drought vulnerability based on socioeconomic and biophysical indicators. *International Journal of Disaster Risk Reduction*, *98*, 104121.

[4] Asrade, T. M., & Yigzaw, G. M. (2025). Spatio-temporal drought monitoring in the Megech–Dirma watershed, Ethiopia, using Google Earth engine. *Scientific Reports*, *15*(1), 45416.

[5] Amal, N. (2023). Hubungan Evapotranspirasi, Hujan dan Elevasi Muka Air Tanah pada Lahan Gambut Tropis Sebagai Awal Penentuan Kondisi Lahan Basah. *Jurnal Ilmu Lingkungan*, *21*(4), 830-838

[6] Putri, R. A., & Novitasari, N. (2022). Analysis Of Drought Index In The Gambut Sub-District, South Borneo, For Wildfire Peatland Mitigation. *Cerucuk*, *6*(3), 207-215.

[7] Supriatna, S., Hashilah, F., Mukhtar, M. K., & Wardani, K. K. (2022). Determinant of land use change in South Kalimantan: An evidence from Banjarbaru City and Banjar Regency. *Forest and Society*, *6*(1), 422-435.

[8] Abdourahamane, Z. S., Garba, I., Boukary, A. G., & Mirzabaev, A. (2022). Spatiotemporal characterization of agricultural drought in the Sahel region using a composite drought index. *Journal of Arid Environments*, *204*, 104789.

[9] Schwartz, C., Ellenburg, W. L., Mishra, V., Mayer, T., Griffin, R., Qamer, F., ... & Tadesse, T. (2022). A statistical evaluation of Earth-observation-based composite drought indices for a localized assessment of agricultural drought in Pakistan. *International Journal of Applied Earth Observation and Geoinformation*, *106*, 102646.

[10] Gaona, J., Quintana-Seguí, P., Escorihuela, M. J., Boone, A., & Llasat, M. C. (2022). Interactions between precipitation, evapotranspiration and soil moisture-based indices to characterize drought with high-resolution remote sensing and land-surface model data. *Natural Hazards and Earth System Sciences Discussions*, *2022*, 1-30.

[11] Liou, Y. A., & Thai, M. T. (2023). Surface water availability and temperature (SWAT): An innovative index for remote sensing of drought observation. *IEEE Transactions on Geoscience and Remote Sensing*, *61*, 1-12.

[12] Wei, W., Zhang, H., Ma, L., Wang, X., Guo, Z., Xie, B., ... & Wang, J. (2022). Reconstruction and application of the temperature-vegetation-precipitation drought index in mainland China based on remote sensing datasets and a spatial distance model. *Journal of environmental management*, *323*, 116208.

[13] Rahman, K. U., Ejaz, N., Shang, S., Balkhair, K. S., Alghamdi, K. M., Zaman, K., ... & Hussain, A. (2024). A robust integrated agricultural drought index under climate and land use variations at the local scale in Pakistan. *Agricultural Water Management*, *295*, 108748.
[14] Alzurqani, S. A., Zurqani, H. A., White Jr, D., Bridges, K., & Jackson, S. (2024). Google Earth Engine application for mapping and monitoring drought patterns and trends: A case study in Arkansas, USA. *Ecological Indicators*, *168*, 112759.
[15] Duan, X., Aslam, R. W., Naqvi, S. A. A., Kucher, D. E., Afzal, Z., Raza, D., ... & Said, Y. (2025). Multi-index assessment and machine learning integration for drought monitoring using google earth engine. *IEEE Journal of Selected Topics in Applied Earth Observations and Remote Sensing*, *18*, 16497-16516.
[16] Khosravi, Y., Homayouni, S., & St-Hilaire, A. (2024). An integrated dryness index based on geographically weighted regression and satellite earth observations. *Science of the Total Environment*, *911*, 168807.
[17] Wei, W., Zhang, X., Liu, C., Xie, B., Zhou, J., & Zhang, H. (2023). A new drought index and its application based on geographically weighted regression (GWR) model and multi-source remote sensing data. *Environmental Science and Pollution Research*, *30*(7), 17865-17887.
[18] Jin, C., Jiang, N., Tian, X., Zheng, E., & Shi, Q. (2024). Analysis of the spatial and temporal evolution of drought in Henan based on a nonlinear composite drought index. *scientific Reports*, *14*(1), 29347.
[19] Zhong, Y., Hong, S., Wei, Z., Walker, J. P., Wang, Y., & Huang, C. (2024). Spatial downscaling of SMAP soil moisture estimation using multiscale geographically weighted regression during SMAPVEX16. *Journal of Hydrology*, *637*, 131348.
[20] Ning, J., Yao, Y., Tang, Q., Li, Y., Fisher, J. B., Zhang, X., ... & Fan, J. (2023). Soil moisture at 30 m from multiple satellite datasets fused by random forest. *Journal of Hydrology*, *625*, 130010.
[21] Crow, W. T., Chen, F., & Colliander, A. (2022). Benchmarking downscaled satellite-based soil moisture products using sparse, point-scale ground observations. *Remote Sensing of Environment*, *283*, 113300.
[22] Chen, H., Yang, N., Song, X., Lu, C., Lu, M., Chen, T., & Deng, S. (2025). A novel agricultural drought index based on multi-source remote sensing data and interpretable machine learning. *Agricultural Water Management*, *308*, 109303.
[23] Satapathy, T., Dietrich, J., & Ramadas, M. (2024). Agricultural drought monitoring and early warning at the regional scale using a remote sensing-based combined index. *Environmental Monitoring and Assessment*, *196*(11), 1132.
[24] Li, J., Li, Y., Yin, L., & Zhao, Q. (2024). A novel composite drought index combining precipitation, temperature and evapotranspiration used for drought monitoring in the Huang-Huai-Hai Plain. *Agricultural Water Management*, *291*, 108626.
[25] Sa'adi, Z., Yusop, Z., Alias, N. E., Shiru, M. S., Muhammad, M. K. I., & Ramli, M. W. A. (2023). Application of CHIRPS dataset in the selection of rain-based indices for drought assessments in Johor River Basin, Malaysia. *Science of the Total Environment*, *892*, 164471.
[26] Chatterjee, S., Desai, A. R., Zhu, J., Townsend, P. A., & Huang, J. (2022). Soil moisture as an essential component for delineating and forecasting agricultural rather than meteorological drought. *Remote Sensing of Environment*, *269*, 112833.
[27] Khosravi, Y., & Ouarda, T. B. (2025). Drought risks are projected to increase in the future in central and southern regions of the Middle East. *Communications Earth & Environment*, *6*(1), 384.
[28] Gumus, K. A., Balcik, F. B., Esetlili, T., & Kahya, C. (2023). Monitoring drought dynamics using remote sensing-based combined drought index in Ergene Basin, Turkiye. *Open Geosciences*, *15*(1).

[29] Başakın, E. E., Stoy, P. C., Demirel, M. C., Ozdogan, M., & Otkin, J. A. (2024). Combined drought index using high-resolution hydrological models and explainable artificial intelligence techniques in Türkiye. *Remote Sensing*, *16*(20), 3799.

[30] Baluch, S. M., Wang, L., Faiz, M. A., Li, H., Chen, Y., Wang, L., & Li, M. (2025). Adaptation simulation and planning for crop yield under climate change: Integrating AquaCrop and DSSAT to project drought-induced yield risks in the Sanjiang Plain. *Agricultural Water Management*, *319*, 109818.